Recent Studies of Hydrogen Negative Ion Source and Beam Production for NBI in Large Helical Device

Recent Studies of Hydrogen Negative Ion Source and Beam Production for NBI in Large Helical Device*)

Katsunori IKEDA, Shaofei GENG[1)], Katsuyoshi TSUMORI, Haruhisa NAKANO, Masashi KISAKI, Kenichi NAGAOKA, Masaki OSAKABE, Osamu KANEKO and Yasuhiko TAKEIRI

National Institute for Fusion Science, 322-6 Oroshi, Toki 509-5292, Japan
[1)]*SOKENDAI (The Graduate University for Advanced Studies), 322-6 Oroshi, Toki 509-5292, Japan*

(Received 7 December 2015 / Accepted 25 February 2016)

The state of hydrogen plasma in the extraction region in a hydrogen negative-ion (H^-) source for NBI has been investigated. We clearly observe an improvement of H^- density owing to the surface production effect with Cs seeding. H^- ions are widely distributed in the extraction region which is obtained by movable cavity ring down (CRD). We confirm a negative ion rich plasma with a few electrons in the extraction region, which state is important for reduction of electron contamination in extracting beam. An extraction area is reached 30 mm from the PG surface, which is measured by a 2D imaging diagnostic for H_α emission. We find the insensitive area for H^- extraction at the PG surface between the apertures. Negative ions produced at the surface are considered to have been supplied in the extraction region. The flow velocity of H^- ions is obtained by a four-pin Langmuir probe using a photodetachment technique with an Nd:YAG laser. H^- ion flows from the plasma grid surface, and its direction drastically changes at 20 mm from the production surface. This flow behavior is considered to be an important characteristic for improving H^- density in the extraction region.

Keywords: NBI, negative ion source, extraction region, negative-ion rich plasma, particle flow

DOI: 10.1585/pfr.11.2505038

1. Introduction

Neutral beam injector (NBI) is an indispensable heating device for production of high-density and hot plasmas in fusion development. We have installed five NBIs in the Large Helical Device (LHD) [1], and have achieved 27 MW beam injection. We use a positive-hydrogen ion (H^+) source in two beam lines (BL) arranged radial injection. High-power (6 MW/BL) with lower energy (40 ∼ 60 keV) beam injection allows effective ion heating [2] and profile measurement of ion temperature [3]. These systems are already upgraded for deuterium operation. We will inject 9 MW deuterium beams from each BL with higher beam energy (60 ∼ 80 keV) in the future deuterium experiment in LHD.

We also use negative-hydrogen ion (H^-) source in the three other BLs, which has been continuously operated since 1998 [4]. These systems inject high-energy neutral beam (180 keV) to LHD with tangential direction. The nominal injection beam power is 5 MW for each BL. We have achieved 6.9 MW beam injection in the first BL using a slot type grounded grid (GG) [5]. The H^- current density has reached 340 A/m^2, which exceeds the target current density for NBI system in ITER (International Thermonuclear Experimental Reactor). According to the Child-Langmuir Law, a current density of H^- ion is proportional to $1/\sqrt{m_i}$ by space-charge limit. Here, m_i is the mass of ion. We expect the extracting current density of D^- ions to be 70% of H^- beam current using the same configuration for the beam accelerator and the same extraction voltage. This is the main problem for D^- operation in negative ion source. For this reason, improvement of the negative hydrogen ion source is required for the deuterium beam operation.

On the other hand, it is considered that H^- ions produced on the PG surface release to the extraction region of the source. The direction of the extraction of H^- ions is opposite to the initial direction of H^- ions. The understanding of this extraction mechanism for H^- ions is the key issue to improve beam current and beam divergence angle. However, this is an unclear region. We have installed many diagnostic devices in the NIFS-RNIS(NIFS R&D Negative Ion Source) [5] to investigate the state of source plasma and the behavior of H^- ions in the extraction region.

In this paper, we will introduce the the configuration of the NIFS-RNIS, and arrangement of the diagnostic devices. We find the negative-ion rich plasma in the extraction region, and the distribution of H^- density is obtained by movable cavity ring-down (CRD) system. Extraction behavior of H^- ions measured by 2D imaging diagnostic is also shown. Finally, we will discuss the charged particle flows and H^- ion temperature estimated by the four-pin

author's e-mail: ikeda.katsunori@lhd.nifs.ac.jp
*) This article is based on the invited presentation at the 25th International Toki Conference (ITC25).

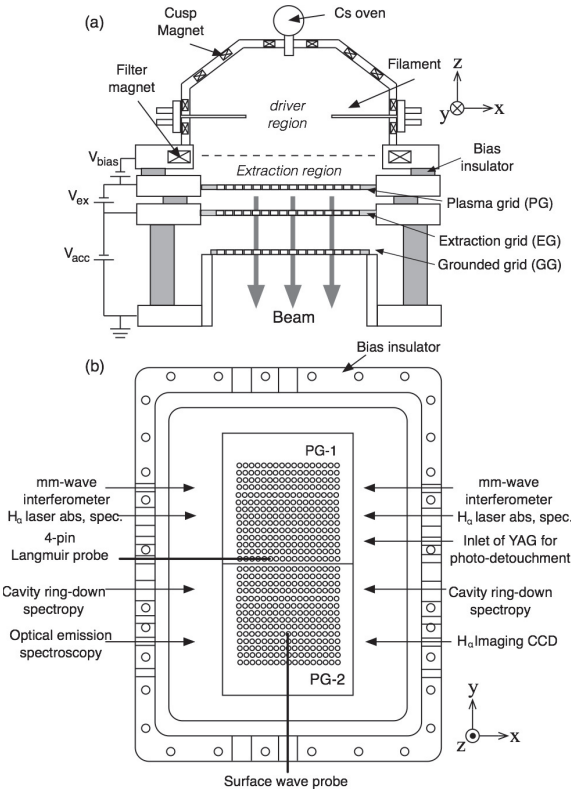

Fig. 1 (a) Schematic drawing of the cross-section of the negative hydrogen ion source (NIFS-RNIS). (b) Arrangement of the diagnostic devices in the extraction region of the source viewing from the back plate.

probe with photo-detachment technique.

2. Configuration of Hydrogen Negative Ion Source and Diagnostic Positions

Figure 1 (a) shows a schematic drawing of the cross-section of the NIFS-RNIS source. The inner dimensions of the arc chamber are 350 mm in width, 700 mm in height, and 230 mm in depth. A hydrogen gas feeder is installed on the side port of the source, and the feeding hydrogen gas pressure is 0.3 Pa in standard operation. We produce hydrogen plasma using arc discharge, which is confined by cusp magnetic field surrounding the arc chamber. A pair of permanent magnets is installed into the filter flange to produce an external magnetic field in front of the plasma grid surface. This horizontally traverse magnetic field is performed to separate the source plasma into two parts called the driver region and the extraction region. We introduce Cesium (Cs) vapor into the arc chamber from the back plate during discharge to produce H^- ions on the PG surface using the surface conversion process. We apply the positive bias voltage ($2 \sim 3$ V in usual operation) on the PG, which performs to reduce electrons in H^- beam.

Figure 1 (b) shows the position of the diagnostic devices viewing from the back plate of the source. All diagnostics are installed on the bias insulator. The center of the diagnostic port is 11 mm far from the PG surface. We use the two segments of molybdenum PG mounting on the copper support frame. Multi-apertures with the diameter of 12 mm open in the PG in an area of 250 mm $\times$ 500 mm. All of the lines of sight from the diagnostic port pass through this area. A cavity ring-down (CRD) [6], a 4-pin Langmuir probe [7], and a surface wave probe [8] use a movable stage to obtain the spatial distributions of target parameters in the extraction region.

H^- ions are extracted through PG apertures, and are accelerated between the extraction grid (EG) and the acceleration grid (GG). The specification of applied voltage of V_{ex} and V_{acc} is 15 kV and 90 kV, respectivey. We also observe the extracted beam current by an ammeter in each power supply and the thermal beam calorimeter array which is located 5 m downstream of the ion source.

3. Observation of Negative-Ion Rich Plasma

Figure 2 (a) shows the typical time trend of the H^- density measured by CRD and the electron saturation current (I_{es}) measured by a Langmuir probe. The hydrogen gas pressure (0.3 Pa) and the arc discharge power (50 kW) are fixed in the experiment. We start Cs seeding with the oven temperature of 185 °C from shot number 75570. The H^- density begins to increase after 15 shots of opening a Cs valve. The H^- density is greatly enhanced to 5 times due to the surface production. We have measured large decrease of the signal intensity of I_{es} into the probe, which indicates that the electron density drastically decreased shot by shot. We also measured the optical emission intensities from hydrogen neutral (H_α : 656 nm, H_β : 486 nm) and the Cs neutral (Cs^0 : 852 nm) as shown in Fig. 2 (b) by the survey spectrometer [9]. The signal intensity of Cs emission which reflects the amount of supplied Cs atoms is also delayed by 15 shots, which is the same as the H^- trend. The time trend of H_α intensity is also similar to the H^- density caused by the excitation process of mutual neutralization which is discussed below.

Figure 3 shows the typical wave form of the current-voltage(I-V) curve measured with a Langmuir probe after Cs conditioning. We have observed a large electron saturation current in the pure volume operation of the source, but it rapidly decreases with Cs seeding. The I-V curve forms to be quite symmetric in the optimal Cs condition for the beam current, which indicates the negative hydrogen ion rich plasma in the extraction region [10]. This symmetric I-V characteristic has been observed in ion-ion plasmas which used chlorine and the C60 [11, 12]. We consider the charge neutrality to be conserved with H^+ and H^- ions with a few electrons lower than 1% in the extraction region of the negative hydrogen ion source. We expect that such a small electron content plays an important role in inhibiting the electron contamination of extracting H^- beam.

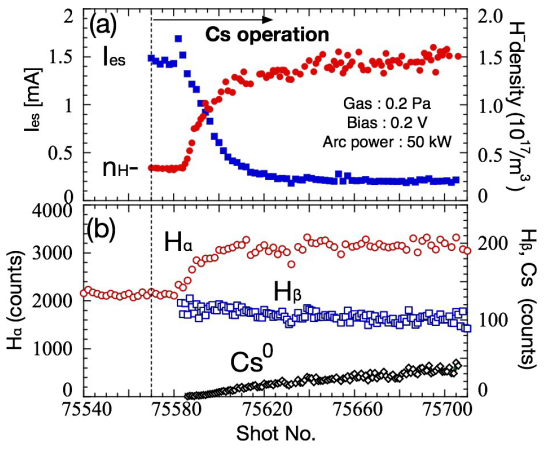

Fig. 2 Typical time trend of H^- density by CRD and the electron saturation current by a Langmuir probe (a) and the optical emission intensity of hydrogen and Cs (b) during Cs conditioning.

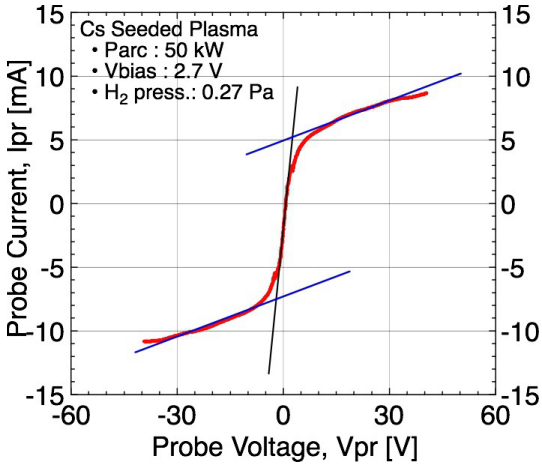

Fig. 3 Typical I-V curve on a Langmuir probe in Cs seeded plasma in the extraction region. The curve has rotational symmetry with respect to the origin.

4. Distribution of H^- Density

The H^- density is measured by the CRD system [6], which is one of the laser absorption diagnostics. We introduce an Nd:YAG laser pulse ($\lambda = 1064$ nm) into the plasma between two high-reflective cavity mirrors set at the bias insulator. The line averaged H^- density is evaluated by the decay time of the laser light attenuated by H^- ions. The accuracy of this measurement depends on the alignment of the laser path and the position of the two cavity mirrors. To measure the distribution of H^- density, we have installed movable drive units with cavity mirrors which are synchronized with the laser path position [13].

Figure 4 (a) shows the typical distribution of the H^- density in the pure volume discharge without Cs. The arc discharge power is 50 kW with 0.3 Pa hydrogen gas pressure. The horizontal axis is the distance from the PG surface (z), and the scannable area is $0\,\text{mm} < z < 27\,\text{mm}$. The H^- density is $4.4 \times 10^{16}\,\text{m}^{-3}$ close to the PG surface,

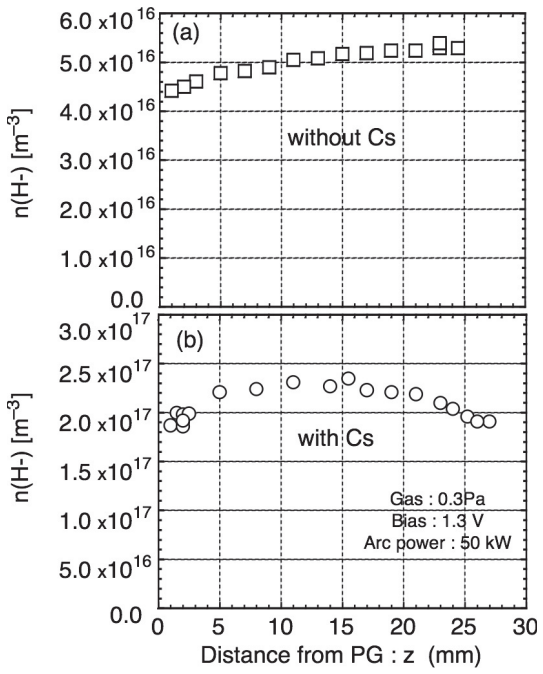

Fig. 4 Typical distribution of H^- density in the pure volume discharge without Cs (a) and the discharge with Cs (b) measured by CRD.

which increases to $5.2 \times 10^{16}\,\text{m}^{-3}$ at $z = 15$ mm. This value increase slightly to the upstream direction. Main contribution of H^- production is considered as the volume production process in the extraction region.

On the other hand, the H^- density improves to $2 \times 10^{17}\,\text{m}^{-3}$ close to the PG surface by Cs seeding as shown in Fig. 4 (b). The distribution in Cs-seeded plasma has a different property for pure volume discharge. The density slightly increases to $2.4 \times 10^{17}\,\text{m}^{-3}$ at $z = 15$ mm, then it decreases to $2.0 \times 10^{17}\,\text{m}^{-3}$ at $z = 25$ mm. These ions are widely distributed in the extraction region of the negative ion source, which is evidence of the production of negative-ion rich plasma in the source. However, this flat distribution is a surprising result because we expected the H^- ions would concentrate close to the PG surface owing to the small Larmor radius of H^- (~ 2 mm). It is expected that there is a flow of H^- ions toward the upstream direction and a mechanism of confining the H^- ion at around $z = 15$ mm around from the PG surface. Understanding of the negative ion distribution formation mechanism requires more detailed study by considering the distribution of electrons and positive hydrogen ions and their charge balance. We also need to know how large is the area for extracting H^- ions in the this region. That will be important information for improving H^- beam current and reducing electron contamination.

5. 2D Distribution for Extraction of Negative Hydrogen Ions

Figures 5 (a) and 5 (b) show the time trace of arc dis-

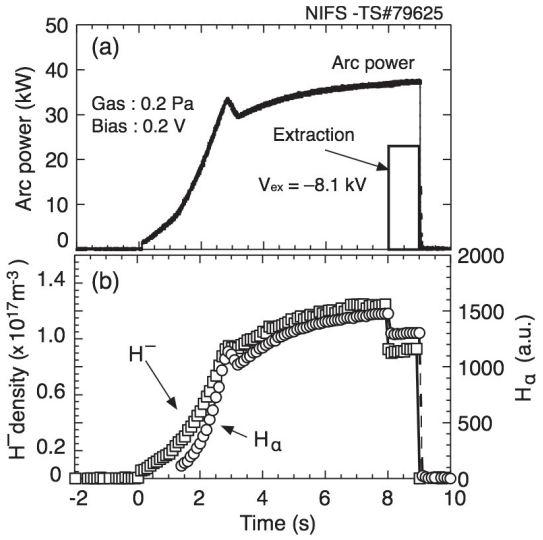

Fig. 5 (a) Time trace of the arc discharge power in H^- source operation. Extraction voltage is applied 1 s at t = 8 s. (b) Time traces of H^- density (open square) and H_α emission intensity (open circle) decrease during beam extraction.

charge power, H^- density, and the intensity of H_α emission after the Cs conditioning. The time duration of the arc discharge is 9 s which power remains constant during 1 s for H^- extraction at the end of the discharge. The temperature of the PG surface varied in the discharge between 180 and 230 °C. The temperatures of the two Cs ovens were controlled at 185 °C in the experiment; the Cs evaporation rate is estimated at 0.17 mg min^{-1} for each oven. The H^- density measured by CRDS at 2 mm from the PG surface increases to 1.25×10^{17} m^{-3} by Cs conditioning from 0.3 $\times 10^{17}$ m^{-3} at pure volume operation. The time trace of the H^- density has a similar wave form with arc discharge power during power increasing phase, and it suddenly decreases during beam extraction as shown in Fig. 5 (b). This is also similar to the sudden decrease found on the H_α emission measured at 11 mm from the PG surface.

According to the study of atomic and molecular processes in hydrogen plasma [14, 15], the dominant excitation mechanisms for H_α emission in low temperature (~ 1 eV) hydrogen plasmas are the dissociative recombination between an electron and a H_2^+, and mutual neutralization between a H^+ and a H^-. Since the excitation cross-sections for two reactions is of the same order, the dominant process depends on the population of H^- ions to electrons in the plasma. The fraction of H^- ions is much larger in the extraction region of H^- source after Cs conditioning. Therefore, the reduction of H_α emission results from the decrease in the excited-state hydrogen population created by the mutual neutralization processes, which in turn results from a decrease in the H^- density. Here the reduction value of the H_α intensity owing to beam extraction is defined as ΔH_α, which is the key value to understand the H^- extraction.

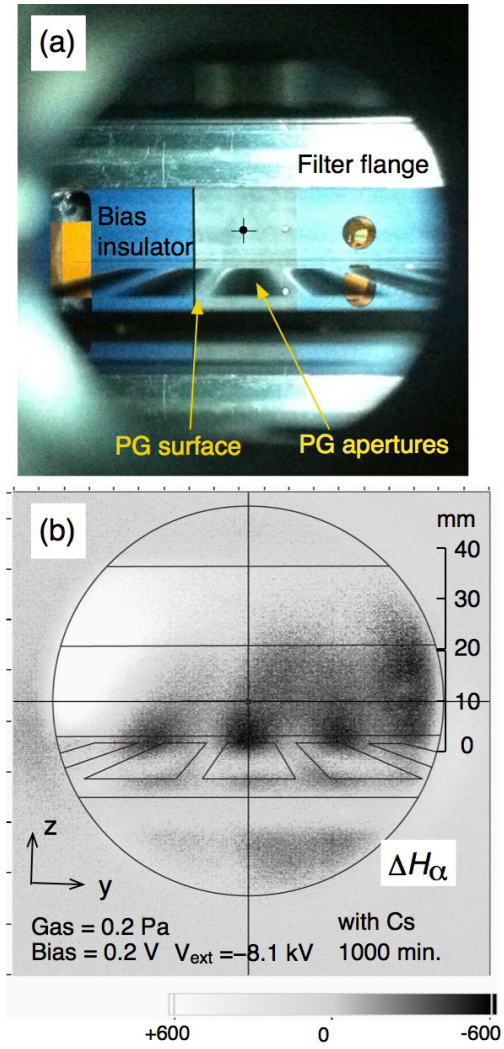

Fig. 6 (a) Field of viewing of the imaging diagnostic for H_α emission. (b) ΔH_α distribution close to the PG surface. Increasing zone, constant zone and decreasing zone is represented in white, gray, and black color. Reproduced with permission from New Journal of Physics, Volume **15**,103026 (2013). Copyright 2013 IOP Publishing and Deutsche Physikalische Gesellschaft.

We install an imaging diagnostic for H_α emission [16] in the extraction region to obtain the 2-dimensional distribution of H^- reduction owing to beam extraction. Figure 6 (a) shows the photograph taken from the viewing port. An area of 35 mm from the PG surface can be observed by the imaging diagnostic. A row of the PG apertures appears as a quadrangle shape in the image because of the shallow angle between the PG surface and the line of sight. Right side is the direction of the center of the ion source, the Cs evaporator is located at 9 cm right from the center of the viewing port. Left side is the the direction of the chamber wall. We produce the ΔH_α image by subtracting the image acquired before beam extraction from the image acquired during beam extraction as shown in Fig. 6 (b). Here the decreased zone, the constant zone, and the growth zone are represent in black, gray, and white,

respectively. We find strong spot-like reductions in the region close to the PG surface (< 10 mm) above the apertures, and these reductions has expand to the inside of the plasma farther than 30 mm in the extraction region. We consider that the distribution of H_α reduction results from the transport of H^- ions owing to the beam extraction. This result leads to the speculation that the negative ion rich plasma are widely distributed in the extraction region because of the optimal Cs conditioning, which is consistent with the flat density distribution measured by CRDS. We also observe the insensitive area for H^- extraction at the surface area between the PG apertures. Negative ions produced at the surface are considered to have been supplied in that region. The reduction distribution is asymmetric in the horizontal directions. The right side of the image is the direction of the source center nearly to the Cs evaporator, where is the intense beam area. The left side of the image is located close to the arc chamber wall where the small beam current area is located. We consider that the asymmetric ΔH_α distribution results from a fraction of the element of H^- ions and electrons due to the different Cs conditioning on the PG surface. This source non-uniformity is considered to be an important issue to improve the H^- source performance toward to the deuterium operation.

6. Observation of Charged Particle Flows

Figure 7 shows the configuration of a four-pin Langmuir probe [7] to obtain an electron flow and an ion flow. The probe tips with the length of 2 mm made by 0.5 mm diameter tungsten wire are set radial on a ceramic stem. Angle of the probe of the next is 90°. The probe works in electrostatic mode at measurement of electron and positive ion flows. We measure the probe current every 30° by rotating the probe. Figure 8 (a) shows the polar distribution of positive saturation current at z = 26 mm. The setting gas pressure and bias voltage is 0.3 Pa and 2.4 V, respectively, in the pure volume plasma with 50 kW arc discharge. We do not apply extraction voltage in this experiment. The distribution of positive saturation current is shifted to the direction of 263° caused by positive ion flow. The flow direction is 83°, which is nearly parallel to the PG surface. The flow velocity in this direction is estimated to be $v = 3.8 \times 10^3$ m/s, as shown in Fig. 8 (b). Positive ion and electron have the same velocity with the same direction. The local magnetic field and the electric field is 0.006 T and 25 V/m, respectively, at z = 26 mm. We calculate the velocity of 4200 m/s in y-direction which is the same order for the measured value. The y component of the flow velocities are the same in three positions. Therefore, we consider that the y component of the flow velocity is due to the crossed field drift. The z component of the flow velocity increases near the plasma grid surface. The observed value of is velocity is −470 m/s at z = 26 mm. The flow velocity in z direction is estimated by collisional diffusion. The flow velocity in z component is to be −240 m/s using the electron mobility of 4 m^2/(Vs) which is consistent of the measured value. Therefore we consider that this flow in z direction is due to ambipolar diffusion.

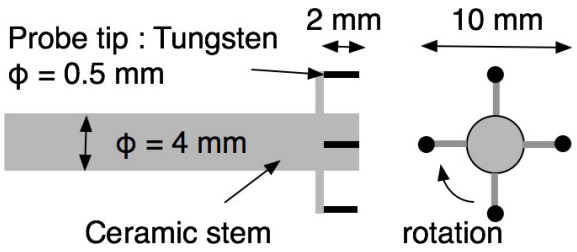

Fig. 7 Dimension of the four-pin Langmuir probe for particle flow measurement. Four probe tip using tungsten wire are radially arranged on the ceramic stem.

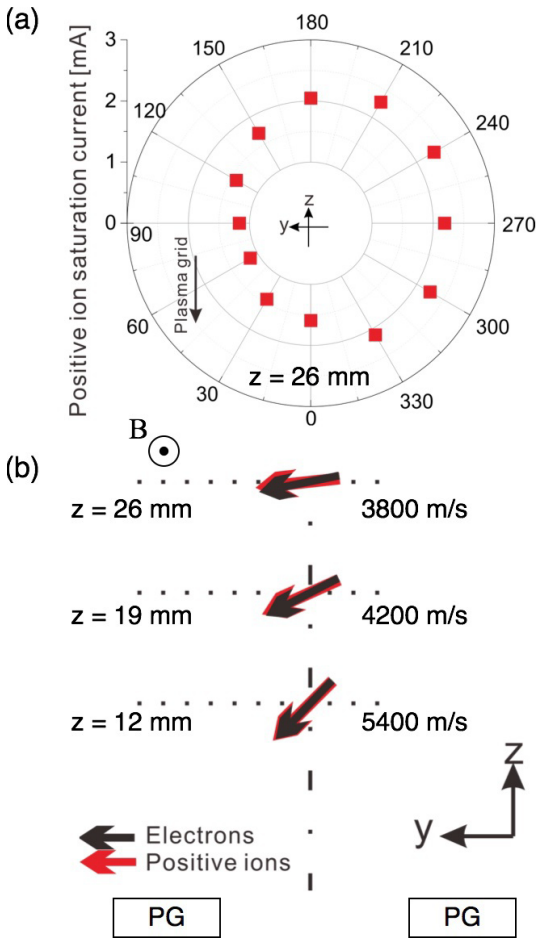

Fig. 8 (a) The polar distribution of positive saturation current pure hydrogen discharge at 26 mm from the PG surface. (b) Flow vectors of proton and electron at PG bias of 2.4 V and 0.3 Pa hydrogen pressure without Cs. The flow velocities are also shown in three positions. Reproduced with permission from Rev. Sci. Instrum. **87**, 02B103 (2016). Copyright 2016 AIP Publishing LLC.

The four-pin Langmuir probe works in photodetachnent mode at H^- flow measurement. Figures 9 (a) and

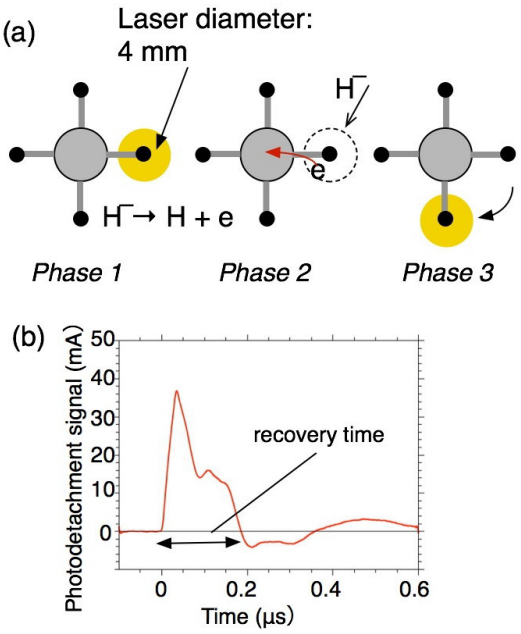

Fig. 9 (a) Illustration of the procedure of H^- flow measurement using photodetachment technique. (b) Typical time trace of the signal intensity of photodetachment electron with recovery time definition. Reproduced with permission from Rev. Sci. Instrum. **87**, 02B103 (2016). Copyright 2016 AIP Publishing LLC.

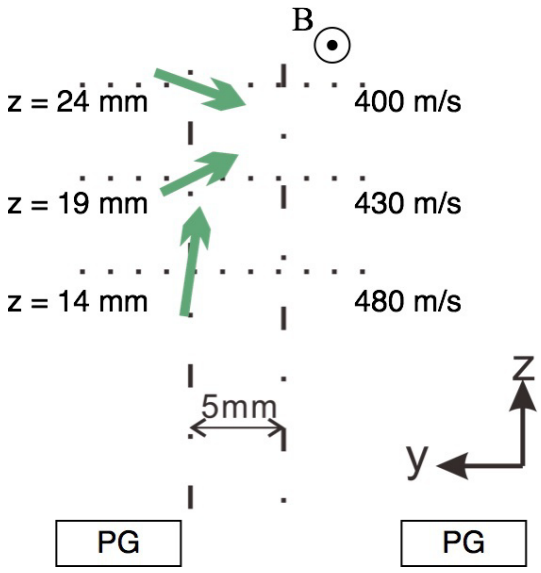

Fig. 10 Flow vectors of H^- at PG bias of 2.4 V and 0.3 Pa hydrogen pressure wit Cs. The flow direction turn in the extraction region and the velocity is ten times smaller than the proton and electron. Reproduced with permission from Rev. Sci. Instrum. **87**, 02B103 (2016). Copyright 2016 AIP Publishing LLC.

9 (b) show the procedure of photo detachment mode and the typical wave form of photodetachment signal, respectively. We use an Nd:YAG laser with the wavelength of 1064 nm, and the beam diameter is 4 mm at the probe tip position. H^- ions are destroyed to a proton and a photo detached electron by irradiated pulse laser around one probe tip at the first phase. In the second phase, the photo detached electrons in the laser column are evacuated by the positive biased probe tip. The signal intensity of the probe rapidly increases by these electrons. Then the surrounding negative ions flow into the detached column to recover the original charge state, the photodetachment signal decreases as shown in Fig. 9 (b). Here we define the charge recovery time as the zero-crossing point of the photodetachment signal. We change the laser position at third phase, and take the photodetachment signal at all positions using the same procedure.

We assume the charge recovery speed is the summation of the thermal velocity and flow velocity of H^- ion. The temperature of H^- ions is obtained by the averaged value of the recovery times. Averaged ion temperature is 0.12 eV at $z = 24$ mm, which is almost the same value estimated in another position. The flow velocity of y direction and z direction is obtained by the subtraction velocity using a pair of probe tips along the y axis and the z axis, respectively. We evaluate the flow vectors of H^- as shown in Fig. 10. The 187° flow direction is observed at $z = 14$ mm, which is opposite to the beam direction. This result might be attributed to the surface produced negative ions on the PG surface. The flow speed is ten times slower than positive ions and electrons. The flow velocities are almost the same in three positions, but the flow directions turn to 246° at $z = 19$ mm, and the direction change to 288° at $z = 26$ mm. This conversion in the flow direction might be the reason for the distribution of H^- ions shown in Fig. 4 (b) in the extraction region. Control of this flow direction will be a key to improve negative hydrogen ion density in the extraction region and to improve the beam current.

7. Summary

In this study the main stress falls on the negative-ion rich plasma which consists of mainly positive and negative ions with a small number of electrons in the extraction region of the hydrogen negative ion source for fusion application. As described in section 3, this plasma is widely distributed in the extraction region of the NIFS-RNIS. The H^- density is 4.0×10^{17} m^{-3} at the 15 mm from the PG surface, these ions are not concentrated close to the PG surface. H^- ions producing on the PG surface by Cs seeding flows to the extraction region, the flow speed is ten times smaller than the thermal speed of H^- ion shown in section 6. We also find the changing of flow direction of H^- about $z = 20$ mm. This flow behavior is considered to be important role for concentrated H^- ions in the extraction region before the beam extraction. We also considered that this H^- flow phenomenon suppresses the electron inflow from the discharge region by space charge compensation, and for keeping low electron contamination in the beam during the beam extraction. As shown in section 5, we ob-

tain the 2D distribution of H^- reduction results from the transport of H^- ions owing to the beam extraction using the reduction distribution of H_α emission. The extraction area for H^- ions is also expanded into the extraction region in negative-ion rich plasma. The insensitive area for H^- extraction is observed at the surface area which result from the production of H^- ions on the PG surface. This result is consistent for the H^- flow measurement.

However, we only measured three positions for H^- flow, and did not extract beams during this experiment. We will apply these flow measurements for charged particle in other position on the PG aperture with beam extraction. This result will be a variable output to know the flow direction of extracting H^- ions and the charged balance on the extraction region during beam extraction. We plan deuterium operation in negative hydrogen ion source in future LHD experiment. We expected further improvement of the negative beam current with low electron contamination in D^- operation by investing and controlling this flow phenomenon in the negative ion source.

Acknowledgements

The authors acknowledge the NBI staff for their technical and operational support. We would like to give heartfelt thanks to Prof. A. Hatayama, Prof. M. Wada, Prof. W. Oohara, Prof. G. Serianni, and Prof. Fantz for discussions and useful comments. This research is supported by JSPS KAKENHI Grant Number 25249134 and the budget for the NIFS No. ULRR702.

[1] Y. Takeiri, O. Kaneko, K. Tsumori *et al.*, Nucl. Fusion **46**, S199 (2006).
[2] K. Nagaoka, H. Takahashi, S. Murakami *et al.*, Nucl. Fusion **55**, 113020 (2015).
[3] M. Yoshinuma, K. Ida, M. Yokoyama *et al.*, Fusion Sci. Technol. **58**, 375 (2010).
[4] Y. Takeiri, K. Tsumori, M. Osakabe *et al.*, AIP Conf. Proc. **1515**, 139 (2013).
[5] K. Tsumori, Y. Takeiri, O. Kaneko *et al.*, Fusion Sci. Technol. **58**, 489 (2010).
[6] H. Nakano, K. Tsumori, K. Nagaoka *et al.*, AIP Conf. Proc. **1390**, 359 (2011).
[7] S. Geng, K. Tsumori, H. Nakano *et al.*, Rev. Sci. Instrum. **87**, 02B103 (2016).
[8] M. Kisaki, K. Tsumori, H. Nakano *et al.*, Rev. Sci. Instrum. **83**, 02B113 (2012).
[9] K. Ikeda, K. Tsumori, U. Fantz *et al.*, AIP Conf. Proc. **1390**, 367 (2011).
[10] K. Tsumori, H. Nakano, M. Kisaki *et al.*, Rev. Sci. Instrum. **83**, 02B116 (2012).
[11] M.V. Malyshev, V.M. Donnelly, J.I. Colonell *et al.*, J. Appl. Phys. **86**, 4813 (1999).
[12] W. Oohara and R. Hatakeyama, Phys. Rev. Lett. **91**, 205005 (2003).
[13] H. Nakano, K. Tsumori, K. Ikeda *et al.*, AIP Conf. Proc. **1515**, 237 (2013).
[14] R.K. Janev W.D. Langer, K. Evance and D.E. Post, *Elementary Processes in Hydrogen-Helium Plasmas* (Springer, Berlin,1987).
[15] U. Fantz and D. Wünderlich, New Journal of Physics **8**, 301 (2006).
[16] K. Ikeda, H. Nakano, K. Tsumori *et al.*, New Journal of Physics **15**, 103026 (2013).